

RESEARCH ARTICLE

Polyacrylic acid ultra-thin films: Influence of cross-linking structure via hyperthermal hydrogen-induced cross-linking

Mengfan Liang¹ | Yan Zhu^{2,3} | Run Xu²  | Junqiang Wang³ | Jian Cui³ | Dequan Yang⁴ | Heng-Yong Nie⁵ | Woon-Ming Lau⁶

¹Xi'an Institute of Electromechanical Information Technology, Xi'an, China

²School of Materials Science and Engineering, Shanghai University, Shanghai, China

³Faculty of Materials Science and Technology, Kunming University of Science and Technology, Kunming, China

⁴Solmont Technology Wuxi Co., Ltd., 228 Linghu Blvd., Wuxi, China

⁵Surface Science Western, The University of Western Ontario, London, Canada

⁶Shunde Graduate School of University of Science and Technology Beijing, Foshan, China

Correspondence

Run Xu, School of Materials Science and Engineering, Shanghai University, Shanghai 200444, China.

Email: runxu@shu.edu.cn

Funding information

Young Talent Fund of Association for Science and Technology in Shaanxi, China, Grant/Award Number: NYHB202221; National Natural Science Foundation of China, Grant/Award Number: 21104028

Abstract

The facile technology of hyperthermal hydrogen-induced cross-linking (HHIC) has recently been employed to efficiently cross-link the typical surface modification material of poly acrylic acid (PAA) on polymer substrates, such as poly-lactic acid substrates, parylene C substrates and hydrophobic polypropylene substrates. This paper systematically studied the HHIC induced self-cross-linking of PAA without polymer substrates. It was found that the —H was cleaved not only from the —C—H, but also from the surface functional group —COOH, evidenced by both X-ray photoelectron spectroscopy (XPS) measurement and the water contact angle test. We explained the self-cross-linking process as a result of both —C—C— bonding and —COOC— bonding. Meanwhile, it was also found that PAA on different substrates can also be cross-linked by secondary electron generated by X-ray radiation during XPS analysis, which could be the main reason for wide variations of different reported XPS results.

KEYWORDS

functionalization of polymers, self-assembly, synthesis and processing techniques

1 | INTRODUCTION

Ultra-thin polymer films can be used as effective modifiers to control the surface properties of different materials. The development of various hybridization and polymerization processes has made it possible to prepare such polymer-based films with a novel structure and special performance. The terminal grafting of polymer chains on various surface has aroused widespread attention because of the formation of different polymer brushes.^{1–3} In the past few years, most studies are focused on the preparation of

polymer films by grafting of the polymer on substrates. However the strong inter-molecular interactions and controlled polymer chains in the cross-linking structure introduce modified properties that are distinguished from those of the bare substrat.^{4–6} The main significance for the application of cross-linking polymer coatings is to adjust the interaction behavior between the surface and external environment.

Poly acrylic acid (PAA) is one of the best candidates for biocompatible materials due to its high concentration of carbocyclic acid (—COOH) functional group and hence

excellent hydrophilic properties. So, PAA have been well investigated due to its potential application in vascular graft,⁷ regenerative medicines,⁸ catheters⁹ and nanogenerator.^{10,11} Recently, polymer bulk bending and surface modification methods have been used to construct a dense barrier structure in the matrix in order to improve the surface properties (such as hydrophilia and adhesion) of PAA.

Previous works have grafted PAA onto substrates using various methods.^{12–23} However, the treatments adopted by most of these reports are not pollution-free. Moreover, pulse microwave plasma CVD, which has been widely employed to deposit PAA layer,^{15–18} may lead to a low COOH group concentration when acrylic acid is used during deposition in the grafting. The cross-linking of PAA thin film can also be obtained by annealing via a photo initiator¹⁵ (e.g., 2,2-dimethoxy-2-phenyl acetophenone [DPA]) or electron beam radiation.¹⁹ However, a complex focusing electron beam in a high vacuum system as a photo initiator for photo-induced cross-linking limits the cross-linking area due to a small electron beam size. Hyperthermal hydrogen-induced cross-linking (HHIC), a relatively new technology with several advantages such as low temperature treatment, both large area and local treatment, without requirement of crosslinking agent and without contamination, can cross-link PAA efficiently and firmly with the polymer substrates, such as PLA substrate,²⁰ PPXC substrate,²¹ and hydrophobic polypropylene substrate.²² Although previous studies focused on cross-linking PAA and polymer substrates, it's worth noting that HHIC can also cause PAA to cross-link by itself.

Additionally, we found that, although x-ray photoelectron spectroscopy (XPS) has been applied to characterize both PAA film and the interface between PAA and substrate, the resulting XPS data were conflicting and inconsistent.²³ Among the most-used four components for C1s peak, for carbon atom in different locations in the PAA molecule, the major inconsistency is C4 component in C1s, 1.7 eV away from the main aliphatic C1s peak due to structurally degraded PAA molecule induced by photoelectrons from the substrate.^{20,24}

Herein, we focused on the growth of ultra-thin PAA layer on Si wafer by spin-coating and the self-crosslinking behavior of as-prepared films by using HHIC method.²¹ The —H is cleaved not only from —C—H, but also from functional group —COOH. The self-cross-linking of PAA are then demonstrated by —C—C and the —COOC—bonding, which was evidenced by both XPS results and the water contact angle test. For the first time, we also found that the cross-linking of PAA can result from secondary electron induced by X-ray radiation during XPS analysis, which are likely the main reason for a wide variation of reported XPS data of PAA.

2 | EXPERIMENTAL SECTION

2.1 | Spin casting deposition of PAA films

The substrates including the Si wafer (about $10 \times 10 \text{ mm}^2$) and the 10 nm Ti foil were firstly sputtered, and then a 100 nm Pt was coated by e-beam evaporation under the working pressure of 2×10^{-7} Torr. Thin films were prepared by spin-coating using a 0.1 to 0.7 wt% PAA solution (MW = 450,000, from Sigma-Aldrich as received) dissolved in ethanol. The thickness of thin films was measured using a Beer–Lambert approach based on the attenuation of signal ratio of C1s of PAA to substrates (e.g., Si 2p or Pt 4f).

2.2 | Cross-linking PAA by using HHIC

Cross-linking experiments were conducted on a home-made electron cyclotron resonance (ECR) enhanced microwave plasma reactor, by using extraction ions to fill a space full with H_2 gas to collide and exchange its kinetic energy to hydrogen. This process may produce H with some certain kinetic energy and/or H_2 with more kinetic energy. The energetic hydrogen breaks bonds in the organic molecular and then some C radicals may cross-link with each other. The bombardment influence of hyperthermal hydrogen on the samples was estimated by the extraction voltage (as primary H^+ kinetic energy) and collision numbers, which depend on the distance between extraction grids, sample surface, and the pressure, for a given extraction voltage. Some of the bombarded PAA samples were soaked and washed by ethanol, and then dried with compressed N_2 . Direct evidence of the cross-linking was to be identified if there was any PAA film remaining in the surface after washing by ethanol.

2.3 | Characterization

X-ray photoelectron spectroscopy (XPS) were carried out with a Kratos Axis Ultra spectrometer using a monochromatic Al $K\alpha$ source (8 mA, 14 kV). High resolution spectra of core-level were recorded using a 0.05 eV step and 20 eV pass energy and an analysis area of $300 \times 700 \mu\text{m}^2$, while survey spectra were recorded at 0.7 eV step and 160 eV pass energy and an analysis area of $300 \times 700 \mu\text{m}^2$. AFM measurement was performed with a Park System (Model: XE-100) operating at tapping mode with which one can capture topography and phase image simultaneously. We used a tapping cantilever with a nominal spring constant

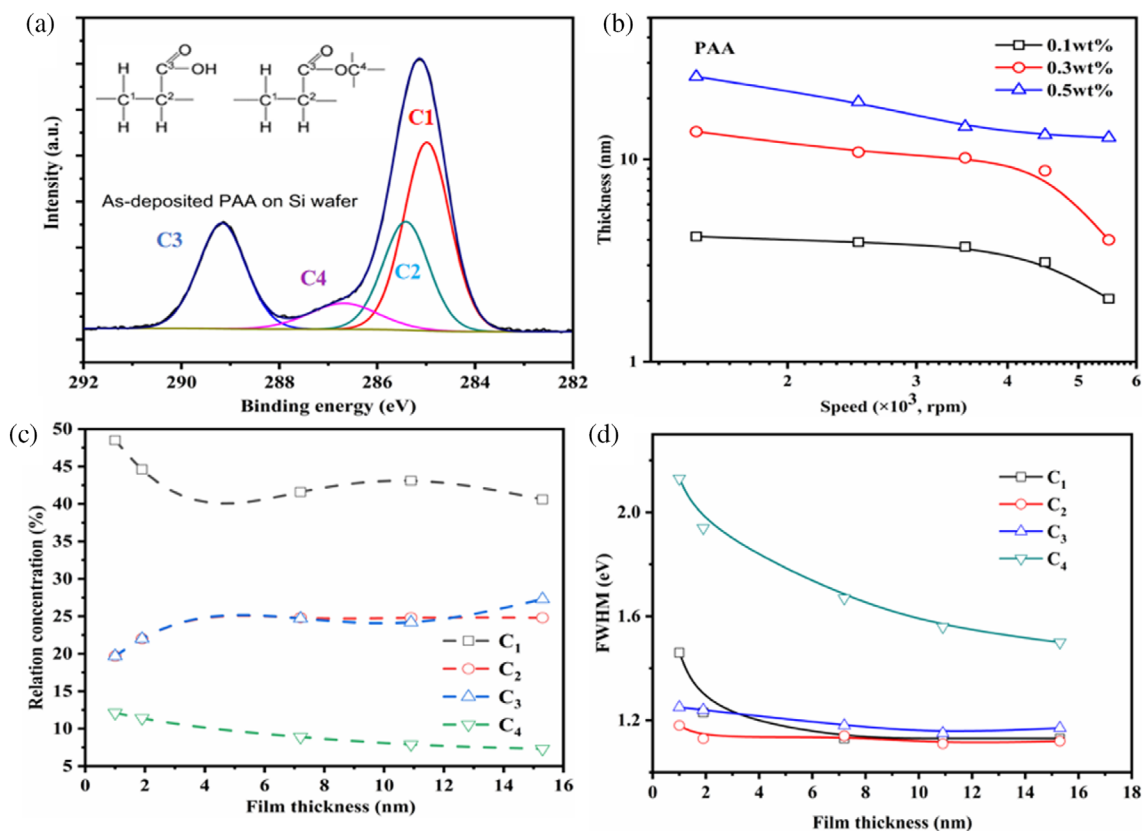


FIGURE 1 (a) Typical high-resolution spectra of X-ray photoelectron spectroscopy (XPS) C1s of the as-deposited poly acrylic acid (PAA) on Si wafer; the inset shows the PAA molecular structure with the indication of C 1 s component. (b) PAA film thickness as a function of spin-coating speed for different PAA concentration; (c) C1s components relative concentration in PAA thin film; (d) variation of C1s components peak full width at half maximum (FWHM) on the film thickness [Color figure can be viewed at [wileyonlinelibrary.com](https://onlinelibrary.wiley.com/doi/10.1002/app.53144)]

of 40 N/m and the tip was pyramidal in shape with a radius of curvature about 20 nm.

3 | RESULTS AND DISCUSSION

3.1 | XPS analysis of PAA thin films

X-ray photoelectron spectroscopy (XPS) has been applied to characterize both PAA film and the interface between PAA and substrate. The XPS survey spectra show that there are only C, O, and Si signals. Typical high-resolution spectra of XPS C1s of the as-deposited PAA on Si wafer (Figure 1a) can be fitted into four components. C1, associated with C-C/C-H bond, is located at 285 eV; C2 is 0.4 eV higher than C1; C3 is 4.2 eV higher than C1; and C4 is 1.7 eV higher than C1, likely coming from the structural degradation of PAA molecule induced by photoelectrons from the substrate.^{20,24} Table 1 summarized the published XPS data about PAA.

The thickness of PAA thin films derived from XPS results as a function of spin-coating speed can be found in Figure 1b. The thickness of the thin film can be

approximately estimated by the C1s to Si2p peak area, using the following equation:

$$\frac{I_{C1s}}{I_{Si2p}} = \frac{I_{C1s}^0}{I_{Si2p}^0} \frac{1 - e^{-d/\lambda_{Si2p}}}{e^{-d/\lambda_{C1s}}} \quad (1)$$

where I present the peak intensity (peak area) of photoelectron emission, d is thickness of the thin films, and λ is the photoelectron mean free path in the thin films. The method was assumed as one of the best methods to estimate the thickness of organic molecular layers.^{25–27}

It seems to fit linear relationship in log–log coordination under the spin coating speed below 4500 rpm, consistent with theoretical model^{28,29}:

$$h = KC_0(\nu_0 D_0)^{1/4} / \omega \quad (2)$$

Where, K is a number of order unity, C , ν , D , and ω are the initial PAA concentration, the kinematic viscosity, the solute diffusivity, and the spin speed, respectively. The dependence of the thin film thickness of PAA on the

Samples	C1 (285)	C2, C3 (285.4, 289.2)	C4 (286.7)	Refs.	
Expected ^a	40	30	30	0	This work
bulk	42	29	29	0	20
Thick layer	42	29	29	0	21
Thin layer on					
Si	66	15	15	3	20
Ti	52	19	19	9	
Fe	54	21	21	4	
Al	48	23	23	6	
Cu	54	18	18	10	
Ni	50	18	19	13	21
glass	39	27	27	7	16
Thick layer	52.8	12.9	12.7	little	20

^aEstimated by PAA molecule formula.

concentration is shown in Figure 1b, which is also well consistent with the Equation (2) and reference 30.

It is worthwhile noting that the relative content of C4 component is slightly decreased with the thickness of the thin films, which may result from a decreased photoelectron induced effect from the substrate as described below. Although we noted that there is little change of C4 peak position, its peak width (FWHM, full width at half maximum), as shown in Figure 1d, is significantly decreased with the increasing of PAA film thickness, probably owing to an increasingly ordered structure of PAA.

To further identify photoelectron induced effect, we then compared two PAA samples with different substrates: Si and Pt (100 nm with 10 nm Ti as interlayer between Pt and Si wafer) coated on Si substrate. The XPS survey spectra of the two samples can be found in Figure 2. A strong background for PAA on Pt can be easily seen in Figure 2a. In other words, there is stronger photoelectron cross-section from Pt than that from Si. Our detailed XPS data shows that the ratio of C4 to C2 (Figure 2b) increases with both radiation time and higher photoelectron yield from the substrates. Indeed, the ratios shows a quickly increasing rate (slope) for the PAA on the Pt substrate, suggesting the stronger damage for the PAA on the Pt substrate. Obviously, the relative concentration of C4 component, due to photoelectron induced cross-linking from $-\text{COOH}$ cleavage of H to form $-\text{COOC}-$,²⁰ is associated with the Si substrate and the thickness of PAA layer for a given X-ray power density. Therefore, we can easily understand the wide variation of those data of the Table 1, which may come from the different PAA thicknesses, substrates and x-ray power densities as well.

The C1s spectra of PAA film bombarded by HHIC can be found in Figure 3a for an 8 nm PAA film on the Si

TABLE 1 The collection of X-ray photoelectron spectroscopy (XPS) C1s components for poly acrylic acid (PAA) from published data (at. %)

substrate. As compared with the untreated sample (Figure 1a), the wider C1s line shape comes from the increased disorder of the chemical bonds during HHIC treatment. Figure 3b summarizes the evolution of C1s component as a function of the treatment time. Clearly, the intensities of C4 and C1 components increase with the treatment time, while the intensities of C3 and C2 components decrease with the treatment time, indicating that there is much more $-\text{C}-\text{C}-$ and $-\text{COOC}-$ formation, and $-\text{COOH}$ group is decreased upon the treatment time. These results indicate that $-\text{H}$ cleaves from $-\text{C}-\text{H}$ and $-\text{O}-\text{H}$, and then both $-\text{COOC}-$ and $-\text{C}-\text{C}-$ bonds form subsequently, finally leading to the cross-linking of original PAA, as shown schematically in Figure 3d.

The PAA thickness estimated by XPS, as a function of the treatment time before and after the washing can be found in Figure 3c. One can see that the PAA thickness keeps constant during the treatment, suggesting the treatment is a very soft treatment and without any etching effects on the PAA film. However, the thickness of PAA film becomes thinner after washing, indicating that un-cross-linked PAA components are always present even after the long treatment time. Also, the PAA thickness (after washing) is increased as the treatment time as shown in Figure 3c, indicating that more and more PAA becomes crosslinked together with increasing HHIC treating time.

3.2 | Surface morphology of PAA film

Atomic force microscopy (AFM) images of the PAA thin film after hyperthermal hydrogen bombardment and ethanol washing are shown in Figure 4. It is demonstrated

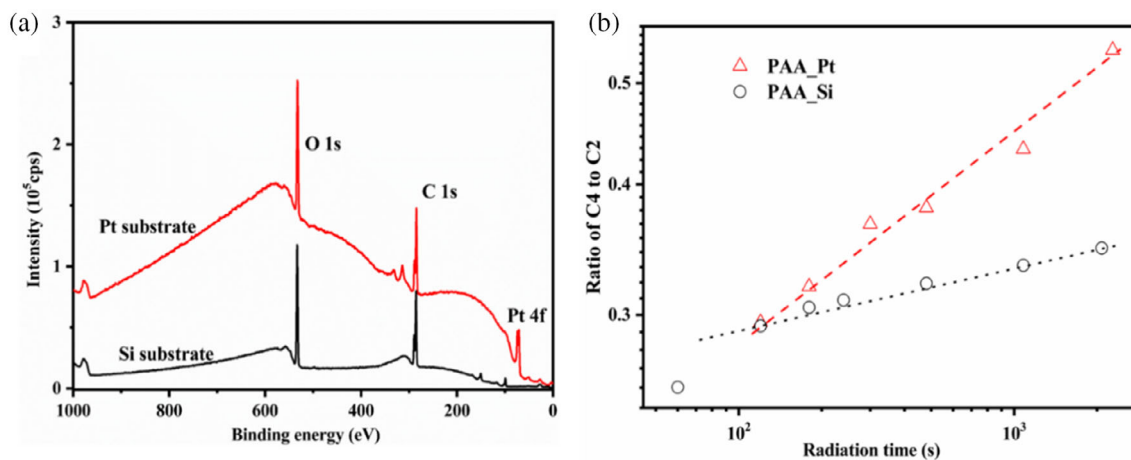


FIGURE 2 (a) X-ray photoelectron spectroscopy (XPS) survey of poly acrylic acid (PAA) films on Si wafer and Pt surface respectively, (b) the ratio of C4 to C2 component as a function of X-ray radiation time (X-ray power is about 48 W, less than general power 140 W) [Color figure can be viewed at [wileyonlinelibrary.com](https://onlinelibrary.wiley.com/doi/10.1002/app.53144)]

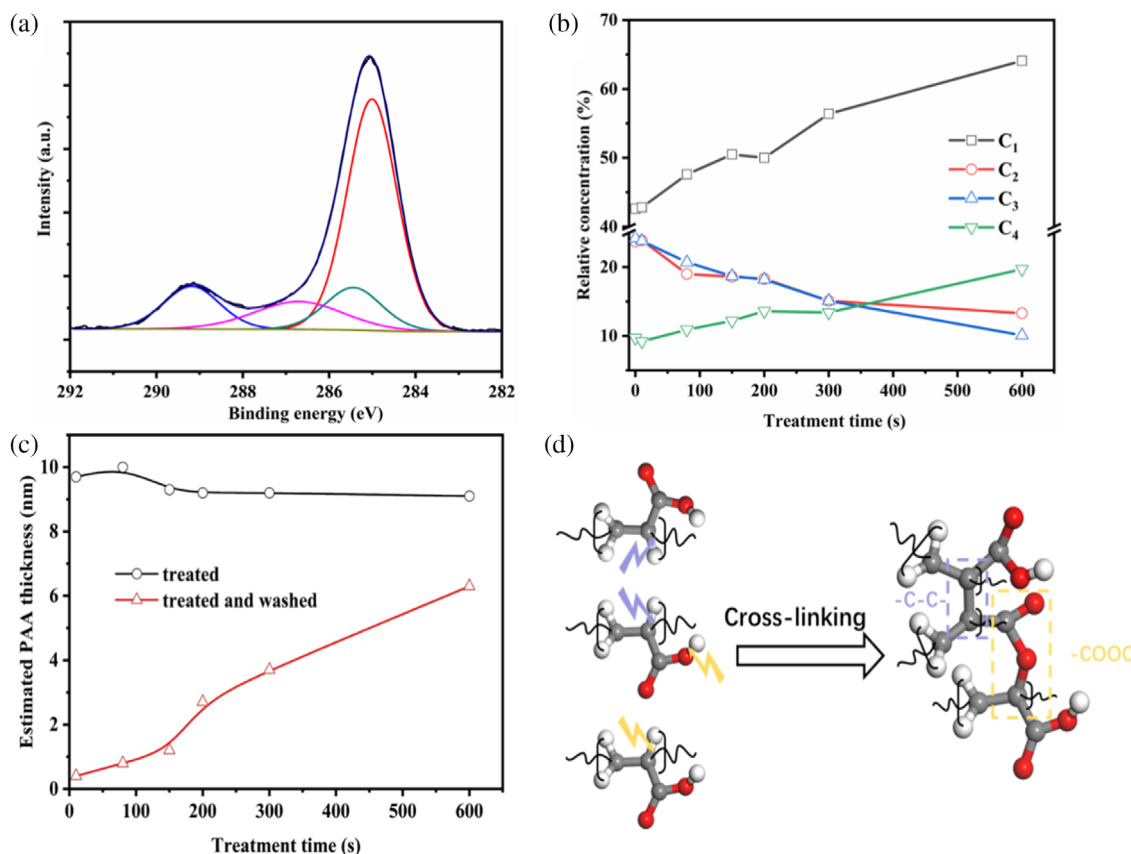


FIGURE 3 (a) C1s X-ray photoelectron spectroscopy (XPS) spectra of poly acrylic acid (PAA) with different treated for 500 s; (b) C1s components of PAA film as a function of the treatment time by HHIC; (c) the estimated PAA thickness as a function of the treatment time before and after washing; (d) mechanism diagram of hyperthermal hydrogen-induced cross-linking (HHIC) [Color figure can be viewed at [wileyonlinelibrary.com](https://onlinelibrary.wiley.com/doi/10.1002/app.53144)]

that the surfaces of PAA are smooth in the nanometer scale even if there are a few bulk particles on the surface for both as-deposited PAA and those after 600 s

treatment time. Moreover, there is no observed change in the AFM topography for the films that has been cross-linked, indicating no decomposition and sputtering of

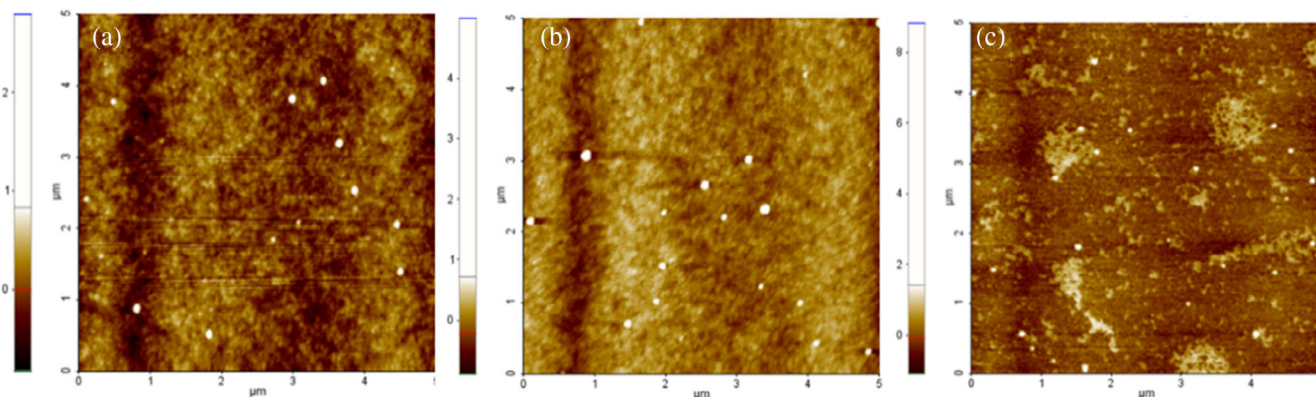


FIGURE 4 Atomic force microscopy (AFM) images of poly acrylic acid (PAA) films on Si wafer with different hyperthermal hydrogen-induced cross-linking (HHIC) treatment: (a) untreated; (b) 600 s + washed, and (c) 100 s + washed [Color figure can be viewed at [wileyonlinelibrary.com](https://onlinelibrary.wiley.com/doi/10.1002/app.53144)]

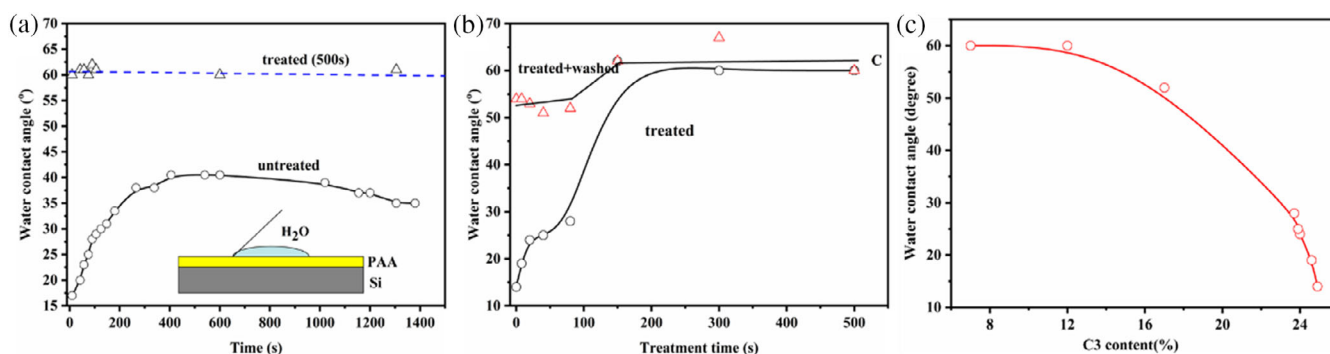


FIGURE 5 (a) Static water contact angle on as-prepared poly acrylic acid (PAA) film as function of water droplet time, (b) treatment time effects on the water contact angle, (c) water contact angle as a function of C3(—COOH) component concentration. All measured are completed within 30 s after droplet on the surface. [Color figure can be viewed at [wileyonlinelibrary.com](https://onlinelibrary.wiley.com/doi/10.1002/app.53144)]

carbon occurring during the hyperthermal hydrogen bombardment, consistent with the XPS measurement (Figure 4). However, there are some clusters or particles on the surface after bombardment and washing, indicating that the PAA without cross-linking has been washed away while the cross-linked PAA will be well retained on the Si wafer surface. Meanwhile, PAA with short treatment time will only leave some PAA on the substrate after washing by ethanol (Figure 4c). In contrast, there is only Si substrate for untreated and washed PAA film in the Si wafer in the AFM image (not shown here), indicating no cross-linking of PAA for untreated samples.

3.3 | Wettability of PAA film surface

One of the direct evidences of surface retained —COOH group can be demonstrated by water static contact angle measurement. It is noted that the contact angle changes with time for as-deposited PAA thin film, as shown by a typical cases in Figure 5a. One can see that the contact

angle is increased upon time within the first 400 s, and then slowly decreased with time. The change of water contact angle for no-cross-linked PAA results from the highly water soluble properties of the PAA. On the other hand, the contact angle of the cross-linked PAA film by HHIC is very stable due to the cross-linking of PAA (Figure 5a). As shown in Figure 5b, the static contact angle of the PAA is also varied with different treatment time. Obviously, the PAA lost its wettability after the cross-linking by HHIC, owing to the loss of the PAA function group —COOH. This is in agreement with XPS results in Figures S1 and 3. The changes of water contact angle, both for the washed and unwashed PAA, are stabilized after 150 s treatment, well consistent with reports from reference 24.

The —COOH group content in the PAA film is supposed to be associated with water contact angle, as shown in Figure 5c. The rapid increasing of water contact angle may be caused by loss of —COOH due to excessive bombardment of hyperthermal hydrogen. Obviously, HHIC of PAA film can result in the breaking of both —C—H

bonds and —O—H bonds, then form the cross-linking (Figure 3d), although it seems that there are much more broken C—H bonds than broken O—H bonds. Indeed, the broken —O—H bonds decrease the number of —COOH groups, which is not expected for the cross-linking.

4 | CONCLUSION

The ultra-thin layer of PAA has been deposited by spin-coating processes and the thickness can be controlled by PAA concentration and the speed of spin-coating. Both the XPS results and the water contact angle measurement evidence the cross-linking of PAA. It is further elucidated that the HHIC induced self-cross-linking of PAA without polymer substrates are therefore via both —C—C— bonding and —COOC— bonding, and the —H atom in PAA molecular is cleaved by HHIC not only from the —C—H, but also from the —COOH functional group. In addition, we also found that secondary electron induced by X-ray radiation during XPS analysis can lead to the cross-linking of PAA, which are likely the main reason for a wide variation of reported XPS data of PAA.

AUTHOR CONTRIBUTIONS

Run Xu: Conceptualization (lead); writing – review and editing (lead). **Mengfan Liang:** Data curation (lead); writing – original draft (lead). **Yan Zhu:** Formal analysis (lead); writing – review and editing (lead). **Junqiang Wang:** Software (lead). **Jian Cui:** Data curation (equal); formal analysis (equal). **Dequan Yang:** Formal analysis (equal); investigation (equal). **Heng-Yong Nie:** Data curation (equal); formal analysis (equal). **Woon-Ming Lau:** Software (equal); validation (equal).

ACKNOWLEDGMENTS

This work was supported by the National Natural Science Foundation of China (grant no. 21104028), the Young Talent Fund of Association for Science and Technology in Shaanxi, China (grant no. NYHB202221), the 2014 Competitive Grant Program of Oversea Returnees Research Projects (Yan Zhu). Special thanks to Mrs Margaret Yau for polishing our manuscript.

CONFLICT OF INTEREST

The authors declare no conflicts of interest.

DATA AVAILABILITY STATEMENT

The data that support the findings of this study are available from the corresponding author upon reasonable request.

ORCID

Run Xu  <https://orcid.org/0000-0003-4686-1765>

REFERENCES

- [1] T. Sato, G. J. Dunderdale, A. Hozumi, *ACS Appl. Polym. Mater.* **2021**, *3*, 1395.
- [2] M. Snelgrove, C. McFeely, K. Shiel, G. Hughes, P. Yadav, C. Weiland, J. C. Woicik, P. G. Mani-Gonzalez, R. Lundy, M. A. Morris, E. McGlynn, R. O'Connor, *Mater. Adv.* **2021**, *2*, 769.
- [3] K. Liu, C. M. Yang, B. M. Yang, L. Zhang, W. C. Huang, X. P. Ouyang, F. G. Qi, N. Zhao, F. G. Bian, *Chinese J. Polym. Sci. (English Ed.)* **2020**, *38*, 92.
- [4] J. Liang, R. Wang, R. Chen, *Polymers (Basel)*. **2019**, *11*, 491. <https://doi.org/10.3390/polym11030491>
- [5] Y. Zhao, G. Li, Y. Gao, D. Wang, Q. Huang, D. Wang, *ACS Energy Lett.* **2019**, *4*, 1271.
- [6] R. K. Hallani, M. Moser, H. Bristow, M. V. C. Jenart, H. Faber, M. Neophytou, E. Yarali, A. F. Paterson, T. D. Anthopoulos, I. McCulloch, *J. Org. Chem.* **2020**, *85*, 277.
- [7] K. Morita, T. Suzuki, Y. Nishimura, K. Matsumoto, C. Numako, K. Sato, M. Nakayama, R. Sasaki, C. Ogino, A. Kondo, *J. Biosci. Bioeng.* **2018**, *126*, 119.
- [8] F. Yang, F. Totsingan, E. Dolan, S. D. Khare, R. A. Gross, *ACS Omega* **2020**, *5*, 4403.
- [9] C. Ngambenjawong, H. Phuengkham, M. Theerasilp, N. Nasongkla, *Proc. IEEE Conf. Nanotechnol.*, Birmingham, UK, **2012**. <https://doi.org/10.1109/NANO.2012.6403799>
- [10] H. G. Menge, N. D. Huynh, H. J. Hwang, S. Han, D. Choi, Y. T. Park, *ACS Energy Lett.* **2021**, *6*, 2451.
- [11] F. Li, H. Wang, X. Ma, *J. Detection Control.* **2021**, *43*, 28.
- [12] Z. Liu, Z. Yin, J. Wang, Q. Zheng, *Adv. Funct. Mater.* **2019**, *29*, 1.
- [13] F. Wang, H. Yang, M. Li, X. Kang, X. Zhang, H. Zhang, H. Zhao, W. Kang, B. Sarsenbekuly, S. Aidarova, M. Gabdullin, *J. Mol. Liq.* **2020**, *314*, 113644.
- [14] J. Sheridan, M. Sonebi, S. Taylor, S. Amziane, *Constr. Build. Mater.* **2020**, *235*, 117536.
- [15] C. Vilani, D. E. Weibel, R. R. M. Zamora, A. C. Habert, C. A. Achete, *Appl. Surf. Sci.* **2007**, *254*, 131.
- [16] S. A. Voronin, M. Zelzer, C. Fotea, M. R. Alexander, J. W. Bradley, *J. Phys. Chem. B.* **2007**, *111*, 3419.
- [17] S. Fraser, R. D. Short, D. Barton, J. W. Bradley, *J. Phys. Chem. B.* **2002**, *106*, 5596.
- [18] R. Severens, J. Bastiaanssen, D. Schram, *Surf. Coatings Technol.* **1997**, *97*, 719.
- [19] I. Saaem, M. Libera, J. Tian, *Bioeng. Proc. Northeast Conf.*, Stony Brook, NY, USA, **2007**. <https://doi.org/10.1109/NEBC.2007.4413365>
- [20] S. R. Leadley, J. F. Watts, *J. Electron Spectros Relat Phenomena* **1997**, *85*, 107.
- [21] H. Shao, Z. K. He, K. Q. Xu, X. Hu, Y. L. Zhou, C. Y. Tang, J. Mei, M. B. Shuai, W. M. Lau, D. Hui, *J. Phys. Chem. C* **2016**, *120*, 28598.
- [22] T. Trebicky, P. Crewdson, M. Paliy, I. Bello, H. Y. Nie, Z. Zhi, X. Fan, J. Yang, E. R. Gillies, C. Tang, *Green Chem.* **2014**, *16*, 1316.
- [23] H. Bennetand, G. J. Oover, *J. Chem. Educ.* **1993**, *70*, A25.

- [24] Z. Zheng, X. D. Xu, X. L. Fan, W. M. Lau, R. W. M. Kwok, *J. Am. Chem. Soc.* **2004**, *126*, 12336.
- [25] P. E. Laibinis, C. D. Bain, G. M. Whitesides, *Silver and Gold. J. Phys. Chem.* **1991**, *95*, 7017.
- [26] C. L. Lamont, J. Wilkes, *Langmuir* **1995**, *15*, 2037.
- [27] X. Wallart, C. Henry de Villeneuve, P. Allongue, *J. Am. Chem. Soc.* **2005**, *127*, 7871.
- [28] W. W. Flack, D. S. Soong, A. T. Bell, D. W. Hess, *J. Appl. Phys.* **1984**, *56*, 1199.
- [29] C. J. Lawrence, *Phys. Fluids* **1988**, *31*, 2786.
- [30] P. Louette, F. Bodino, J.-J. Pireaux, *Surf. Sci. Spectra* **2005**, *12*, 54.

SUPPORTING INFORMATION

Additional supporting information can be found online in the Supporting Information section at the end of this article.

How to cite this article: M. Liang, Y. Zhu, R. Xu, J. Wang, J. Cui, D. Yang, H.-Y. Nie, W.-M. Lau, *J. Appl. Polym. Sci.* **2022**, *139*(46), e53144. <https://doi.org/10.1002/app.53144>